Comparison of several modulation strategies for the Four Switch Buck-Boost converter

Víctor Díaz
Power Electronics Systems Group
Carlos III University of Madrid
Av Univeridad 30 28911
Leganes Madrid
victor.diaz@uc3m.es

Andrés Barrado
Power Electronics Systems Group
Carlos III University of Madrid
Av Univeridad 30 28911
Leganes Madrid
andres.barrado@uc3m.es

Antonio Lázaro
Power Electronics Systems Group
Carlos III University of Madrid
Av Univeridad 30 28911
Leganes Madrid
alazaro@ing.uc3m.es

Pablo Zumel
Power Electronics Systems Group
Carlos III University of Madrid
Av Univeridad 30 28911
Leganes Madrid
pzumel@ing.uc3m.es

***Abstract*—The Four Switch Buck-Boost converter (FSBB) is a widely used topology for DC-DC applications in which isolation is not required. This is mainly due to its bidirectionality, and the ability to operate under a wide range of input and output voltages. There are several modulation strategies for this converter, each one with its strengths and weaknesses.**

In this paper, several modulators from state of the art are compared, and the losses of the transistors and the inductor are computed. With this information, it is intended to select the best modulator depending on the input and output voltages, output power, and hardware limitations of the designed FSBB.

Keywords—FSBB, Modulator, ZVS, ZCS, pulse width modulation (PWM), DC-DC.

I. INTRODUCTION

The Four Switch Buck-Boost converter (FSBB) is a widely used DC-DC converter with a variety of applications. It is used in PV systems because it works with a wide range of input and output voltages [1]–[3]. It is also commonly used in smart grids due to its bidirectionality [4]. In essence, this converter acts as a buck converter in series with a boost converter [5]. This guarantees the opportunity to work with a wide range of input and output voltages. Furthermore, it reduces the number of components and increases the performance as compared to similar DC-DC converters [6].

The primary bridge of the FSBB (S_1 and S_{1N}) can be considered to control the buck stage of the converter, whereas the second bridge (S_2 and S_{2N}) would be the boost stage. Switch S_1 would control the buck gain of the converter with a duty cycle equal to d_1 , and S_{1N} would function as complementary. S_2 would control the boost stage with a duty cycle d_2 , with S_{2N} working as its complementary. This functioning mode would result in the general formula illustrated in (1). Notice that (1) is not affected by the phase shift ϕ between the bridges, this provides an additional control variable in the system.

In this paper, several modulations for the FSBB converter from state of the art will be studied and compared. In section II several modulations will be presented. In section III, the hardware limitations of each modulator are studied. Section IV will compare the different modulation strategies, and section V will derive some conclusions from this study.

This Work has been partially supported by the Spanish Ministry of Science, Innovation, and Universities through the research project HIDRON (PID2020-116500RB-I00 / AEI / 10.13039/501100011033), and by the European Union-NextGenerationEU/PRTR, the Community of Madrid, and MCIN / AEI / 10.13039/501100011033 through the research project GREENH2CM.

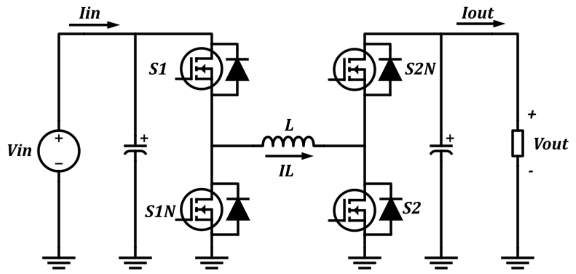

Fig. 1. Four Switch Buck-Boost converter (FSBB)

$$G_v = \frac{V_{out}}{V_{in}} = \frac{d_1}{1-d_2} \quad (1)$$

II. MODULATION STRATEGIES

A. 1 Mode Modulation (1MM)

The simplest type of modulation can be achieved by matching d_1 and d_2 so that they can be expressed as $d_1 = d_2 = D$, equation (1) could then be simplified as follows:

$$G_v = \frac{D}{1-D} \quad (2)$$

In this type of modulation S_1 and S_2 are turned on and off simultaneously for a time $t_1 = D \cdot T$, where T is the period of the Pulse Wide Modulation signal (PWM), and S_{1N} and S_{2N} are activated with the complementary signals. The current through the inductor can be seen in Fig. 2A, where:

$$I_L = \frac{I_{out}}{1-D} \quad (3)$$

$$\Delta i_L = \frac{V_{in} \cdot D \cdot T}{L} \quad (4)$$

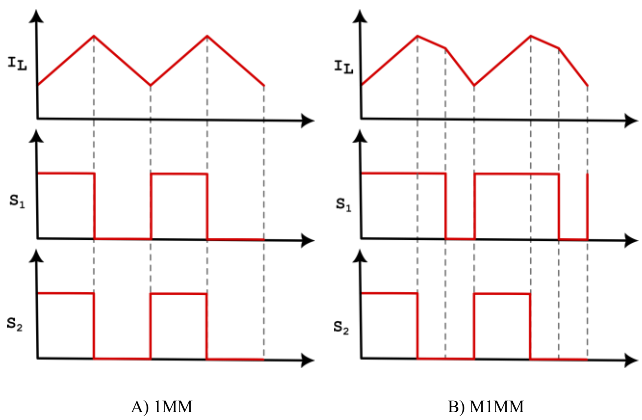

Fig. 2. 1MM waveforms

It can be deduced from (3) that the bigger the D is, the larger the average current through the inductor (I_L) will be.

To reduce the current in the inductor, a new modulation was developed in [7], where d_1 is set to be constant at all times, and d_2 controls the converter, Fig. 2B. The constant value for d_1 must be one that allows the converter to reduce the voltage for the worst case, that is:

$$d_1 = \frac{V_{out}(Min)}{V_{in}(Max)} \cdot \left(1 - d_2(Min)\right) \tag{5}$$

According to (5), if d_2 is allowed to reach zero, then d_1 must be equal to $G_v(Min)$. This would mean that the transfer function of the converter would then be as follows:

$$G_v = \frac{G_v(Min)}{1 - d_2} \tag{6}$$

This modulation then makes the system's control as if it were a boost converter with a certain gain, making the control easier than other modulators. This approach is intended to reduce the current through the inductor. Substituting (6) in (3) (where $d_2 = D$) we obtain (7), the new current through the inductor.

$$I_L = I_{out} \cdot \frac{G_v}{G_v(Min)} \tag{7}$$

With (3) and (7) it can be deduced that this new modulation strategy will only reduce the current through the inductor whenever equation (8) is met.

$$G_v(Min) \geq D \tag{8}$$

Analysing (8), it can be seen that this modulation strategy improves the original only when $G_v(Min)$ is greater than D, so I_L is lower than in the original modulation. It also illustrates that the lower G_v is, the smaller the region where the new modulation improves the original.

B. Buck-Boost mode

To reduce the average current through the inductor, the FSBB converter can be operated as a buck or as a boost converter. If S_2 is set to be always off and, therefore, S_{2N} is constantly closed ($d_2 = 0$), then the converter would work as a buck converter where:

$$G_v = d_1 \tag{9}$$

$$I_L = I_{out} \tag{10}$$

$$\Delta i_L = \frac{(V_{in} - V_{out}) \cdot d_1 \cdot T}{L} \tag{11}$$

If, on the other hand, S_1 is constantly conducting ($d_1 = 1$), then the converter would work as a boost converter where the second branch commutes with a duty cycle of d_2. The converter then will work as:

$$G_v = \frac{1}{1 - d_2} \tag{12}$$

$$I_L = \frac{I_{out}}{1 - d_2} \tag{13}$$

$$\Delta i_L = \frac{V_{in} \cdot d_2 \cdot T}{L} \tag{14}$$

In this case, there are two different modulation strategies (2MM), as seen in Fig. 3A. Working with this kind of modulation would present some instabilities in the region where $V_{in} \simeq V_{out}$. Since S_1 (operating as boost converter) and S_{2N} (operating as buck converter) would always be conducting in this region, or with a very small duty cycle, the control ability of the converter is lost. To resolve the instabilities in this region, several studies have proposed different solutions. In [8] different digital approximations are compared to solve the instability of the buck-boost region, nevertheless, all of them present discontinuities in the transfer function of the converter and must be corrected by abrupt changes in the duty cycle, this makes the control stage more challenging.

In [5] and [9] d_1 is fixed to a constant value D whenever the converter is working in buck-boost mode, generating a 3 Mode Modulation (3MM), Fig. 3B.

It solves the problem of instabilities whenever $V_{in} \simeq V_{out}$, however, this means that when the converter moves from Buck-Boost mode to Boost mode d_1 will abruptly change from D to 1, to maintain the G_v constant d_2 must then change in accordance to (1). As in the previous case, this introduces an oscillation in the system that must be dealt with by the control system.

Similarly to the previous case in [10] and [11], one of the control variables is fixed in this solution, but in this case d_1 is fixed only when the converter is operating in Buck-Boost mode in step-up conditions, but in step-down mode d_2 is fixed instead, resulting in 4 Mode Modulation (4MM), Fig. 3C.

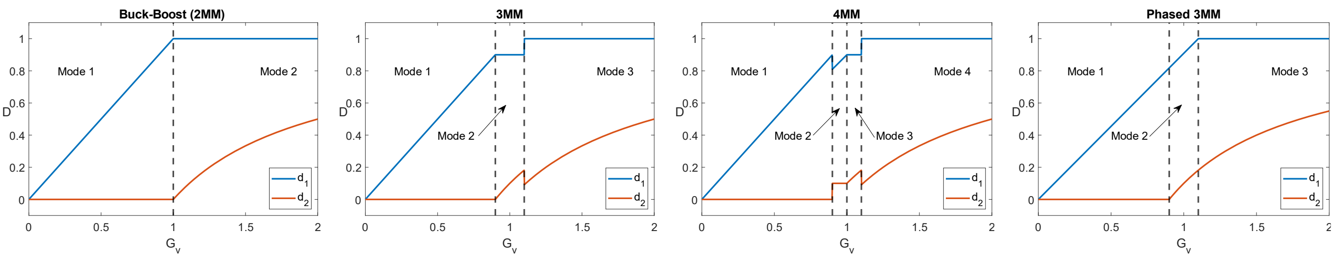

A) B) C) D)

Fig. 3. Relation between d_1 and d_2 with G_v

This is aimed at reducing the inductor current in Buck-Boost mode. It also avoids working with very small duty cycles that may be challenging for the driver stage. However, it presents discontinuities changing from one mode to another.

Working with this 4MM there is an extra control variable, the phase shift between the two bridges (ϕ). In [12] a study on the efficiency of the converter in a 4 Mode modulation depending on ϕ is presented, where the efficiency of the converter is best around $\phi = 180°$.

Lastly, to resolve the discontinuity problems in [13] and [14] a modulator with two carrier signals is proposed, Fig. 4. This allows a smooth transition between the three working modes by phasing the two transfer functions (Ph3MM). It avoids any discontinuities and prevents sudden changes in the duty cycle, Fig. 3D.

C. Reduced switching losses

In the previous section, all modulations were aimed to reduce the average current through the inductor without considering the transistors. In these modulations transistors S_1 and S_2 have hard switching, significantly increasing the power losses and, therefore, temperature. There are two approaches to reduce power losses in the transistors, Zero Current Switching (ZCS) modulation and Zero Voltage Switching (ZVS) modulation.

In [15], two extra transistors and another inductor are introduced in the converter to achieve ZCS. Although these extra components withstand less power and are, therefore, smaller, this topology adds components to the converter and makes the design more complex and expensive.

Another way of reducing power losses is with ZVS modulation. To accomplish this in [16] a modulation is presented where a negative current is induced in i_L to achieve soft switching in S_1 and S_2. The frequency of the signal in this converter must vary to allow sufficient time for the current to reach the necessary negative value, as seen in Fig. 5A and 5B. The frequency variation would make it necessary to design the components for the worst-case scenario at the lowest frequency. It would mean that the inductor losses would get more significant as the frequency increases.

To resolve the variable frequency issue, in [17] an extra stage is added to the modulation, where S_{1N} and S_2 are conducting, so there is a "free-wheeling current" through the inductor (Fig. 5C and 5D) and maintains this state until the period T ends.

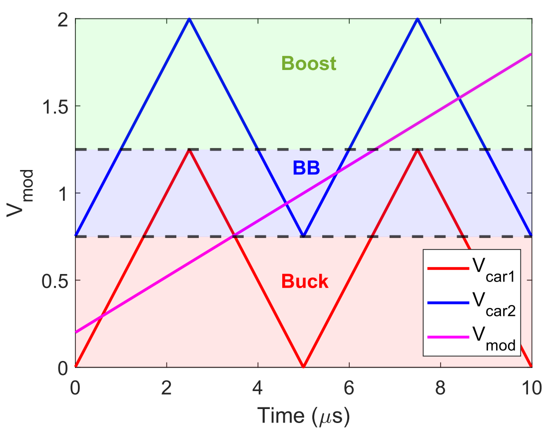

Fig. 4. Modulation strategy for phased 3MM

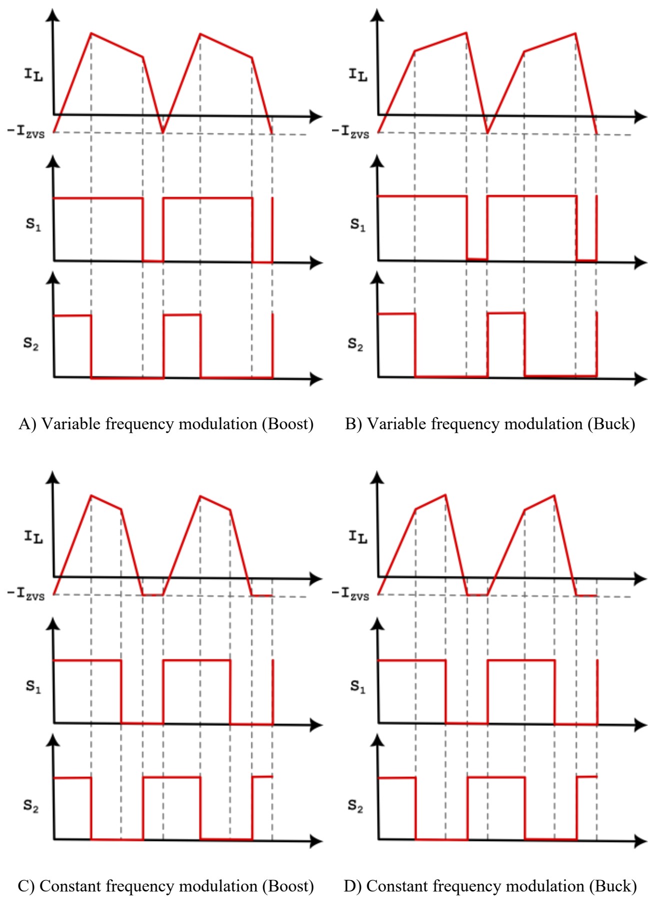

Fig. 5. Waveforms of modulations with soft switching

Since the publication of [17] in 2009, several papers have proposed modifications to this modulation to improve certain characteristics. In [18]–[21], the overall efficiency of the converter is studied and the RMS current through the inductor is minimized using different strategies. Furthermore, in [22] the freewheeling current through the inductor is reduced in order to minimize the conduction losses of both transistors and inductor.

The computation needed to achieve this kind of modulation is very high, so the general control strategy implies implementing a Look-Up Table (LUT). This LUT has three input parameters, V_{in}, V_{out} and I_{out}. The resulting LUT is huge for a wide range of input and output voltages. In [23]–[25], some strategies are used either to reduce the size of the LUT (modifying the 3D LUT to a 2D LUT), or by removing the LUT and changing it for a complex digital strategy.

Nevertheless, even though the modifications improve the modulation, they all stay very similar to that originally proposed in [17].

III. HARDWARE LIMITATIONS

Considering all these types of modulations, up to eight, it can be difficult to decide which strategy must be used in each case. Firstly, it is necessary to check each modulation mode's characteristics to see if it can be implemented in the hardware.

A. Bootstrap

It is quite common to power the upper driver of a half-bridge branch using a bootstrap configuration. Thus, the power is provided by a capacitor that is charged whenever the upper transistor is open and then supplies the power when the transistor is in conduction mode.

Since the power consumption of the MOSFET gate can be neglected after the switching transient, the bootstrap capacitor only needs to store enough energy to charge the parasitic capacitor of the gate (C_{iss}) up to the threshold voltage. This statement is true whenever the half-bridge branch is switching, but if the upper transistor is set to be constantly conducting (to operate as a boost converter, for instance), then the assumption that the consumption is neglectable is no longer true. It means that the capacitor will eventually discharge, opening the transistor and causing the system to malfunction.

To solve this problem, the upper part of the branch must be powered by an isolated power source that provides power at a constant rate. Although this power supply does not pose any technical challenge, it requires some extra components, including a transformer, that will increase both the volume and the price of the final product. Therefore, in applications where a bootstrap is implemented, either for budget reasons or to improve the converter's power density, no modulation that requires one of the transistors to be driving at all times can be selected (2MM, 3MM, 4MM, 3MM in phase).

B. *Duty cycle*

There is another limitation when using a driver with a bootstrap or with an auxiliary power supply. Whenever the duty cycle is near zero, the driver cannot properly switch the transistors. If D is close to 0, and if the driver is not well designed, it may not have enough time to charge the gate capacitor, so the transistor will not conduct.

This means that in some modulations (2MM, 3MM, and Ph 3MM) there are instability areas whenever d_1 or d_2 are close to zero, for instance in 3MM, this limitation would be in d_2 when changing from buck to buck-boost mode.

To solve this issue, there are two possible solutions. A faster driver can be implemented, reducing the gate resistance, or changing the driver. In this case, some antiparallel diodes can be included in the circuit, with adequate characteristics, so they conduct whenever the duty cycle is very small.

C. *Inductor Current*

Sensing the input and output currents and voltages is needed to control and protect the converter. These sensors can have a low cut-off frequency in a DC-DC converter, depending on the application.

Nevertheless, when working with modulations that achieve ZVS (both constant and variable frequency), it is necessary to detect when the inductor current is equal to $-I_{ZVS}$ for switching the second bridge. To achieve this, an extra current sensor is needed in series with the inductor. This sensor needs to have a higher cut-off frequency to detect the actual value of the current. It can be achieved in different ways, usually connecting a sensor in series with S_{2N} like in [18] to avoid the necessity of an insulated sensor.

As in the previous case, although this modification is quite easy to implement, it increases the price of the converter and its volume.

D. *Selection*

Considering only the system's hardware limitations, a number of modulators can be eliminated.

- **Bootstrap**: If the driver is implemented with a bootstrap configuration 2MM, 3MM, 4MM, and phased 3MM cannot be implemented.
- **Inductor current sensor**: If no sensor is added to measure the current through the inductor both modulators that achieve ZVS cannot be implemented.
- **Minimum duty cycle**: If the duty cycle has a limitation as to the smallest value it can achieve (different from 0), then the 2MM, 3MM, and phased 3MM cannot be achieved.

A summary of this comparison can be seen in Table I.

IV. Efficiency Comparison

Considering there are no hardware limitations, an analysis of the efficiency of each modulation has been carried out. To do so firstly an inductor is selected for each modulation. Later, the average current through the inductor is compared to end with an efficiency comparison.

A. *Inductor selection*

Depending on the modulation strategy, the inductor is selected differently. For all modulations that do not achieve soft switching (1MM, M1MM, 2MM, 3MM, 4MM, and Ph3MM), the inductor is selected so that the current ripple is small but still optimizing the inductor size.

On the other hand, for the modulations that allow achieving soft switching (Vf ZVS and ZVS), the inductor current must reach $-I_{ZVS}$ in all cycles. L must be computed as shown in equation (15) to fulfil this requirement.

$$L \leq \frac{V_{in}^2 \cdot V_{out}^2}{2 \cdot P_{out} \cdot (V_{in}^2 + V_{out} \cdot V_{in} + V_{out}^2)} \cdot T \qquad (15)$$

Table I. Modulations Comparison

	Achievable with Bootstrap	Need I_L sensor	D close to zero	Soft Switching	Average I_L	I_L Ripple	I_L RMS	Constant frequency
1MM	Yes	No	No	No	High	Low	$\approx I_L(Avg)$	Yes
M1MM	Yes	No	No	No	High	Low	$\approx I_L(Avg)$	Yes
2MM	No	No	Yes	No	Low	Low	$\approx I_L(Avg)$	Yes
3MM	No	No	Yes	No	Low	Low	$\approx I_L(Avg)$	Yes
4MM	No	No	No	No	Low	Low	$\approx I_L(Avg)$	Yes
Ph 3MM	No	No	Yes	No	Low	Low	$\approx I_L(Avg)$	Yes
Vf ZVS	Yes	Yes	No	Yes	High	High	$\gg I_L(Avg)$	No
ZVS	Yes	Yes	No	Yes	High	High	$\gg I_L(Avg)$	Yes

Also, to ensure that soft switching can be achieved in all ranges of power and voltages, L must be computed using the maximum output power and the minimum voltages. When working with variable frequency, the parameter T must be selected as the smallest one allowed.

For the parameters shown in Table II, an inductor of 5.1µH was selected for non-soft switching modulations to ensure a current ripple lower than 20%. For all modulations that achieve soft switching L must be equal to 0.481µH according to the data in Table II and (15), adding a 10% safety margin.

B. Inductor Current

As seen in previous sections, the main goal of most modulations is to reduce the average current through the inductor, to reduce the losses in both the inductor transistors. This reduction can be seen in Fig. 6, where the 1MM and the Modified 1MM have higher currents than ZVS and 2MM.

The difference between the 2MM, 3MM, 4MM, and the phased 3MM is located only in the region where $V_{in} \simeq V_{out}$, since in the buck and boost modes all strategies work in the same matter. In Fig. 7 a detail of the buck-boost region can be seen, where the 2MM is the one that results in the smallest current. Since the 2MM cannot be achieved due to instabilities, the phased 3MM is the one that results in the lower average current.

C. Efficiency Comparision

A comparison of all the different modulations is carried out to study the operation points in which each strategy is more efficient. The number of modulations has been reduced to ease the comparison. Firstly, between the modulations 1MM and M1MM the latter is studied since the inductor current is significantly lower. Then, of all the modulations with various working modes, the one achievable with the lowest inductor current is the Ph3MM. Lastly, a modulation with ZVS is also compared.

The efficiency of the converter has been computed analytically, using the MATLAB tool. The power losses of the transistors are computed following [26]. On the other hand, inductor losses are computed following [27] and [28]. This comparison has been studied for nominal input voltage, and all possible combinations of output power and voltages.

This comparison is illustrated in Fig. 8, where, as expected, M1MM is the modulation with the lowest efficiency since it has the highest current through the inductor.

It can be seen that in the buck-boost area ($V_{in} \simeq V_{out}$) the efficiency of the Ph3MM drops. This is because for this modulation, this is the only area where all transistors are switching, therefore, the switching losses increase. On the other hand, the ZVS modulation has lower switching losses, but since the current ripple is much higher, the power losses through the inductor increase significantly.

Since for the ZVS modulation the current ripple minimizes in the buck-boost region, this modulation has a higher efficiency whenever the power, and therefore the current, is low. This means that if no hardware limitation is considered, the best modulation for the FSBB would be the Ph3MM. Although, if the converter is working exclusively on buck-boost mode and with low currents, the ZVS modulation is best.

TABLE II. CONVERTER RATINGS

V_{out}	$V_{in}(Min)$	$P_{out}(Max)$	T
$45V - 60V$	$30V - 60V$	$0W - 2.8kW$	$5\mu s$

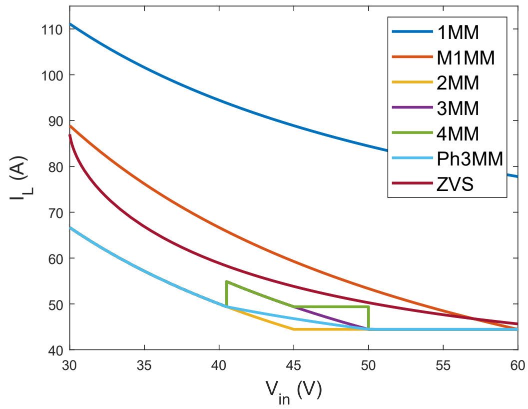

Fig. 6. Average current through the inductor for different modulations. V_{out}=45V; P_{out}=2000W

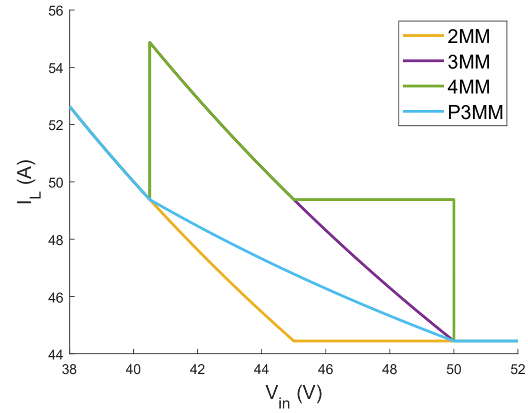

Fig. 7. Average current through the inductor for different modulations, Buck-Boost detail. V_{out}=45V; P_{out}=2000W

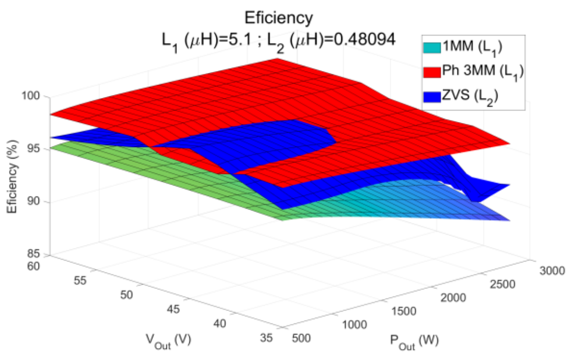

Fig. 8. Efficiency comparison with V_{in}=45

V. CONCLUSION

In this paper, several modulations have been studied and compared. Starting from the simplest modulation (1MM), several papers have been presented illustrating different modifications to improve the system's efficiency. Some of these modulations aimed to reduce the inductor current (M1MM, 2MM, 3MM, 4MM and Ph3MM), while others aimed to reduce the losses in the transistors (Vf ZVS, ZVS).

Later, some hardware limitations were presented for each of the modulations. Finally, all modulations were compared. Firstly, a study of the current through the inductor was presented, to end with an efficiency examination of the most relevant ones. It was concluded that the best modulations are the Ph3MM and the ZVS, depending on the working conditions of the converter.

REFERENCES

[1] C.-W. Chen and Y.-M. Chen, 'Analysis of the series-connected distributed maximum power point tracking PV system', in *2015 IEEE Applied Power Electronics Conference and Exposition (APEC)*, Mar. 2015, pp. 3083–3088. doi: 10.1109/APEC.2015.7104791.

[2] M. Kasper, D. Bortis, T. Friedli, and J. W. Kolar, 'Classification and comparative evaluation of PV panel integrated DC-DC converter concepts', in *2012 15th International Power Electronics and Motion Control Conference (EPE/PEMC)*, Sep. 2012, p. LS1e.4-1-LS1e.4-8. doi: 10.1109/EPEPEMC.2012.6397403.

[3] M. Orellana, S. Petibon, B. Estibals, and C. Alonso, 'Four Switch Buck-Boost Converter for Photovoltaic DC-DC power applications', in *IECON 2010 - 36th Annual Conference on IEEE Industrial Electronics Society*, Nov. 2010, pp. 469–474. doi: 10.1109/IECON.2010.5674983.

[4] H.-S. Lee and J.-J. Yun, 'High-Efficiency Bidirectional Buck–Boost Converter for Photovoltaic and Energy Storage Systems in a Smart Grid', *IEEE Trans. Power Electron.*, vol. 34, no. 5, pp. 4316–4328, May 2019, doi: 10.1109/TPEL.2018.2860059.

[5] X. Ren, X. Ruan, H. Qian, M. Li, and Q. Chen, 'Dual-edge modulated four-switch Buck-Boost converter', in *2008 IEEE Power Electronics Specialists Conference*, Jun. 2008, pp. 3635–3641. doi: 10.1109/PESC.2008.4592520.

[6] M. Schulz, N. Schleippmann, K. Gosses, R. Chacon, and B. Wunder, 'Four Switch Buck/Boost Converter to Handle Bidirectional Power Flow in DC Subgrids', in *PCIM Europe digital days 2020; International Exhibition and Conference for Power Electronics, Intelligent Motion, Renewable Energy and Energy Management*, Jul. 2020, pp. 1–8.

[7] Y. Wang, J. Lan, X. Huang, T. Fang, X. Ruan, and M. Dong, 'An Improved Single-mode Control Strategy Based on Four-switch Buck-Boost Converter', in *2020 IEEE Applied Power Electronics Conference and Exposition (APEC)*, Mar. 2020, pp. 320–325. doi: 10.1109/APEC39645.2020.9124612.

[8] M. Fernandez, A. Rodriguez, M. Rodríguez, A. Vazquez, P. Fernandez, and M. Arias, 'Smooth-Transition Simple Digital PWM Modulator for Four-Switch Buck-Boost Converters', *Electronics*, vol. 11, no. 1, Art. no. 1, Jan. 2022, doi: 10.3390/electronics11010100.

[9] X. Ren, X. Ruan, H. Qian, M. Li, and Q. Chen, 'Three-Mode Dual-Frequency Two-Edge Modulation Scheme for Four-Switch Buck–Boost Converter', *IEEE Trans. Power Electron.*, vol. 24, no. 2, pp. 499–509, Feb. 2009, doi: 10.1109/TPEL.2008.2005578.

[10] L. Callegaro, M. Ciobotaru, D. J. Pagano, E. Turano, and J. E. Fletcher, 'A Simple Smooth Transition Technique for the Noninverting Buck–Boost Converter', *IEEE Trans. Power Electron.*, vol. 33, no. 6, pp. 4906–4915, Jun. 2018, doi: 10.1109/TPEL.2017.2731974.

[11] H. Qin, Y. Yang, S. Xie, W. Chen, J. Peng, and D. Fu, 'Mechanisim of Duty Cycle Mutation and a New Mode Smooth Switching Control Method in High Efficiency Four-Mode Four-Switch Buck-Boost Converter', in *2022 International Conference on Power Energy Systems and Applications (ICoPESA)*, Feb. 2022, pp. 304–311. doi: 10.1109/ICoPESA54515.2022.9754390.

[12] Y. Bai, Z. Zhu, Z. Yang, S. Zha, and S. Hu, 'Analysis and Comparison of Inductor Current Characteristics for Non-Inverting Buck-Boost Converter With Four-Mode Modulation', in *2022 IEEE 5th International Electrical and Energy Conference (CIEEC)*, May 2022, pp. 2534–2540. doi: 10.1109/CIEEC54735.2022.9846753.

[13] Y.-J. Lee, A. Khaligh, and A. Emadi, 'A Compensation Technique for Smooth Transitions in a Noninverting Buck–Boost Converter', *IEEE Trans. Power Electron.*, vol. 24, no. 4, pp. 1002–1015, Apr. 2009, doi: 10.1109/TPEL.2008.2010044.

[14] I. Aharon, A. Kuperman, and D. Shmilovitz, 'Analysis of Dual-Carrier Modulator for Bidirectional Noninverting Buck–Boost Converter', *IEEE Trans. Power Electron.*, vol. 30, no. 2, pp. 840–848, Feb. 2015, doi: 10.1109/TPEL.2014.2315993.

[15] H. Yun, M. Dong, Y. Jian, J. Wan, M. Shen, and Y. Wang, 'Application of soft-switching technology in four switch Buck-Boost circuit', in *2017 12th IEEE Conference on Industrial Electronics and Applications (ICIEA)*, Jun. 2017, pp. 1675–1679. doi: 10.1109/ICIEA.2017.8283108.

[16] K. Xia, Z. Li, Y. Qin, Y. Yuan, and Q. Yuan, 'Minimising peak current in boundary conduction mode for the four-switch buck–boost DC/DC converter with soft switching', *IET Power Electron.*, vol. 12, no. 4, pp. 944–954, 2019, doi: 10.1049/iet-pel.2018.5689.

[17] S. Waffler and J. W. Kolar, 'A Novel Low-Loss Modulation Strategy for High-Power Bidirectional Buck $\bm +$ Boost Converters', *IEEE Trans. Power Electron.*, vol. 24, no. 6, pp. 1589–1599, Jun. 2009, doi: 10.1109/TPEL.2009.2015881.

[18] Z. Zhou, H. Li, and X. Wu, 'A Constant Frequency ZVS Control System for the Four-Switch Buck–Boost DC–DC Converter With Reduced Inductor Current', *IEEE Trans. Power Electron.*, vol. 34, no. 7, pp. 5996–6003, Jul. 2019, doi: 10.1109/TPEL.2018.2884950.

[19] T. Mao, Z. Guo, and S. Mu, 'Soft Switching Control Strategy of Four-Switch Buck-Boost Converter for High Efficiency', in *2022 IEEE International Power Electronics and Application Conference and Exposition (PEAC)*, Nov. 2022, pp. 226–231. doi: 10.1109/PEAC56338.2022.9959120.

[20] Q. Liu, Q. Qian, M. Zheng, S. Xu, W. Sun, and T. Wang, 'An Improved Quadrangle Control Method for Four-Switch Buck-Boost Converter With Reduced Loss and Decoupling Strategy', *IEEE Trans. Power Electron.*, vol. 36, no. 9, pp. 10827–10841, Sep. 2021, doi: 10.1109/TPEL.2021.3064074.

[21] Z. Yu, H. Kapels, and K. F. Hoffmann, 'Extreme High Efficiency Non-Inverting Buck-Boost Converter for Energy Storage Systems', in *PCIM Europe 2016; International Exhibition and Conference for Power Electronics, Intelligent Motion, Renewable Energy and Energy Management*, May 2016, pp. 1–8.

[22] Q. Liu, Q. Qian, B. Ren, S. Xu, W. Sun, and H. Li, 'A New Modulation Strategy for Four-switch Buck-boost Converter with Reduced Freewheeling Current', in *2020 IEEE Applied Power Electronics Conference and Exposition (APEC)*, Mar. 2020, pp. 2104–2108. doi: 10.1109/APEC39645.2020.9124107.

[23] L. Tian, X. Wu, C. Jiang, and J. Yang, 'A Simplified Real-Time Digital Control Scheme for ZVS Four-Switch Buck–Boost With Low Inductor Current', *IEEE Trans. Ind. Electron.*, vol. 69, no. 8, pp. 7920–7929, Aug. 2022, doi: 10.1109/TIE.2021.3104616.

[24] J. Fang, X. Ruan, X. Huang, R. Dong, X. Wu, and J. Lan, 'A PWM Plus Phase-Shift Control for Four-Switch Buck-Boost Converter to Achieve ZVS in Full Input Voltage and Load Range', *IEEE Trans. Ind. Electron.*, vol. 69, no. 12, pp. 12698–12709, Dec. 2022, doi: 10.1109/TIE.2021.3135522.

[25] F. Liu, J. Xu, Z. Chen, R. Huang, and X. Chen, 'A Constant Frequency ZVS Modulation Scheme for Four-Switch Buck-Boost Converter with Wide Input and Output Voltage Ranges and Reduced Inductor Current', *IEEE Trans. Ind. Electron.*, pp. 1–10, 2022, doi: 10.1109/TIE.2022.3187591.

[26] D. D. Graovac, M. Pürschel, and A. Kiep, 'MOSFET Power Losses Calculation Using the Data- Sheet Parameters'. Infineon, 2006.

[27] X. Nan and C. R. Sullivan, 'An improved calculation of proximity-effect loss in high-frequency windings of round conductors', in *IEEE 34th Annual Conference on Power Electronics Specialist, 2003. PESC '03.*, Jun. 2003, vol. 2, pp. 853–860 vol.2. doi: 10.1109/PESC.2003.1218168.

[28] R. W. Erickson and D. Maksimović, *Fundamentals of Power Electronics.*, 2nd ed. Secaucus, NJ, USA: Kluwer Academic Publishers, 2000.